TÜBİTAK

Turkish Journal of Earth Sciences

http://journals.tubitak.gov.tr/earth/

Research Article

Turkish J Earth Sci
(2021) 30: 1151-1161

doi:10.3906/yer-2105-13

Simulation and parametric study on a novel modified Kalina cycle

Guobin LEI[1,*], Jun ZHOU[1], Shengchao SHI[1], Fuzhi QI[1], Jiawei XU[1], Jie PENG[1], Jiaqi ZHANG[2], Dongxi LIU[2], Qingyao MENG[2]

[1]State Grid Qinghai Electric Power Company, Qinghai, China

[2]Key Laboratory of Efficient Utilization of Low and Medium Grade Energy, MOE, Tianjin University, Tianjin, China

Received: 09.05.2021 • **Accepted/Published Online:** 27.09.2021 • **Final Version:** 01.12.2021

Abstract: To improve the utilization rate of hot dry rock resources, it is necessary to recover the energy of geothermal tailwater and improve the net output work. An improved ammonia-water power cycle is proposed based on the Kalina cycle. Taking the geothermal parameters of the Husavik Power Plant in Iceland as the prototype (the water temperature of the geothermal well is 122 °C, and the tailwater temperature is 80 °C), the numerical simulation of the modified Kalina cycle is carried out by using Engineering Equation Solver software. The result shows that the net power output of the modified Kalina cycle increases by 10.5% compared to that of the Kalina cycle. In addition, the parametric study shows that the optimal ammonia concentration of the basic solution in the general area is 0.9. The lower the cooling water temperature is, the lower the turbine exhaust pressure and the higher the net power output. When the ammonia concentrations of the basic solution are 0.6, 0.7, 0.8 and 0.9, the optimum pressures are 29 bar, 36 bar, 41 bar and 45 bar, respectively. The results of this study will contribute to the utilization of geothermal energy in hot dry rock.

Key words: Hot dry rock, Kalina cycle, power cycle, ammonia-water mixture

1. Introduction

As a kind of geothermal resource with large reserves, high temperature and environmental friendliness, the efficient development and utilization of hot dry rock will help to improve the supply structure of renewable energy in China (Li and Wang, 2015). With the in-depth development of hot dry rock exploration, the development and utilization of hot dry rock (HDR) resources is gradually increasing. A series of popularized power cycles are used to improve integrated efficiency, and it is usually found that the power generation cycle is selected to match with (HDR) resources. Wei recommended a hot dry rock power generation system model based on the conventional Kalina cycle (Wei et al., 2015). Meanwhile, others of the HDR power generation cycle mainly include transcritical cycle technology, ORC systems with nonazeotropic mixtures. Among them, the Kalina cycle has been widely studied because of the advantage of the variable temperature phase change characteristics of ammonia-water working media. For these power generation systems, El-sayed and Tribus compared the Rankine cycle and the Kalina cycle and pointed out that the thermal efficiency of the Kalina cycle increases by 10%~20% compared to that of the Rankine cycle (El-sayed and Tribus, 1985). Kalina pointed out that the Kalina cycle had a higher power output than the Rankine cycle with isobutene as the working medium in the same geothermal resource (Bo et al., 1989a, 1989b; Lu et al., 1989; Kalina et al., 1991; Hettiarachchi HDM et al., 2007). Wang studied the merits and disadvantages of the Kalina cycle and Rankine cycle. The performance of the Kalina cycle is better than that of the Rankine cycle without considering the type of heat sources (Wang et al., 2008). Therefore, the literature survey shows that the Kalina cycle can achieve a higher power output from a specified geothermal heat source than the organic Rankine cycle. For Kalina cycle system, Marston pointed out that the temperature of the separator and the turbine inlet pressure are the key factors in optimizing the Kalina cycle (Marston et al., 1994). Zhang (Zhang et al., 2007) studied the thermodynamic properties of ammonia-water mixtures and the thermal performance of the Kalina cycle. Fu proposed a cascade utilization system including the Kalina cycle during the oil production process, and the economic efficiency was improved (Fu et al., 2013).

A series of ammonia-water power cycles based on the Kalina cycle was proposed by other researchers. Wu and Zheng analyzed some combined cycles based on the Kalina cycle with an ammonia-water mixture as the working

* Correspondence: 1072334568@qq.com

medium (Zheng et al., 2002; Wu et al., 2003). Liu and Xu proposed a novel power and refrigeration combined cycle, and the cycle was analyzed and optimized by thermal efficiency and exergetic efficiency as indicators (Liu et al., 2006; Xu et al., 2014). Zheng proposed a new refrigeration and heating system that combined geothermal and solar energy through an ammonia absorption cycle, and the influence of heat source temperature on the refrigeration and heating efficiency was studied (Zheng and Zheng, 2005). Liu and Chen optimized the ammonia absorption refrigeration system using the pinch analysis method and pointed out that the performance coefficient increased by 11.58% (Chen et al., 2012; Liu and Yin, 2012). The ammonia-water power cycles are varied, and the performance can accurately reflect the power generation capacity of the system. However, most of the research stays in the simulation of Kalina cycle system, and there are very few experimental research and demonstration projects.

Currently, several Kalina power plants are in operation throughout the world. Among them, the most famous Kalina geothermal power plant is in Husavik (Ogriseck S, 2009) in which the temperature of geothermal water from the well is approximately 122 °C, the temperature of tail water is approximately 80 °C, and the actual power output is approximately 1950 kW (Nasruddin et al., 2009). The basic schematic of the Kalina cycle of this power plant is shown in Figure 1. Adopting the Husavik power plant as a prototype, the modified Kalina cycle (MKC) is proposed and validated in this paper. In addition, a simulation and parametric study on MKC are carried out, and a comparison between the Kalina cycle power plant and MKC is made.

2. Description and modeling

2.1. Description

According to the actual parameters of the Kalina cycle in Iceland, the temperature of tailwater is approximately 80 °C, and the amount of energy is still contained. Therefore, a district heating system is developed, and good economic benefit is achieved in Iceland. In general regions, the temperature of district heating can be reduced from 80 °C to 60 °C or even lower. Based on the premise of satisfying district heating, some measures can be adopted to decrease the temperature of geothermal tail water for the target to increase the power output. It is possible to increase the net power output by recycling and reinjecting the energy contained by tailwater into the power cycle with some measures. Based on the Kalina cycle, an absorption heat transformer is coupled with the Kalina cycle to decrease the tail temperature and increase the net power.

An absorption heat transformer is a kind of system that can transfer energy from a low-grade heat source to a high-grade heat source (Fang and Luo, 2008; Huang

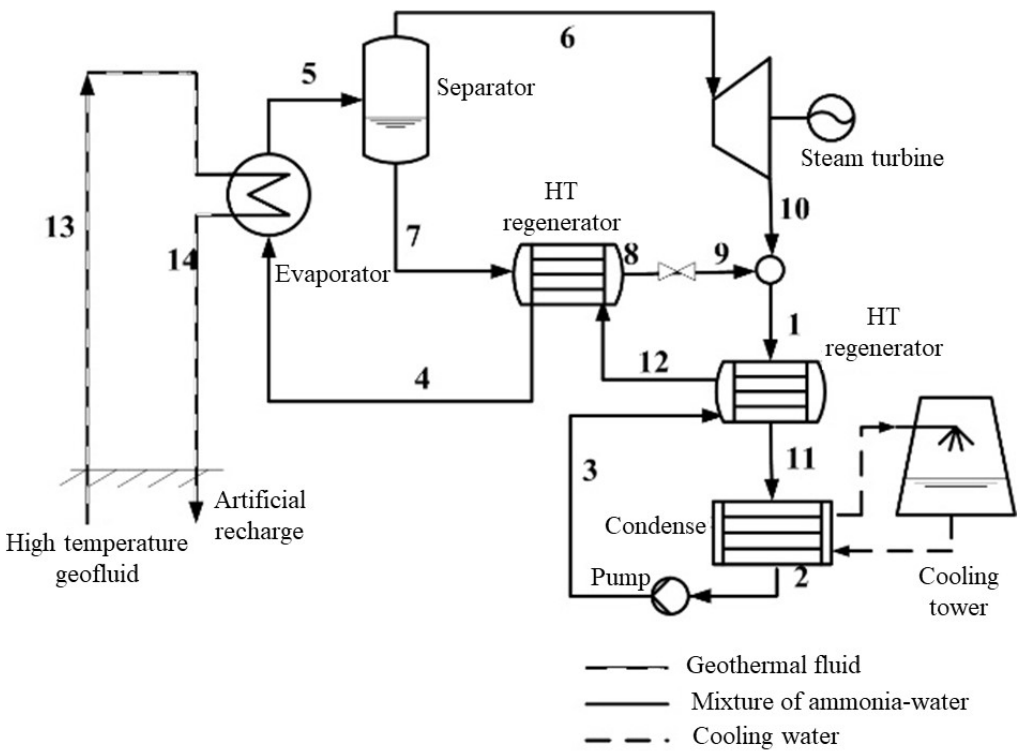

Figure 1. Schematic diagram of KCS.

T and Dong, 2008; Gao et al., 1993). It is possible to recycle tailwater at 80 °C because the temperature of the driven heat source used by the ammonia absorption heat transformer is generally only approximately 50~90°C. Consequently, the MKC is possible in theory. Based on the theory, the schematic diagram of MKC is developed as shown in Figure 2 in which the improved parts are shown in a black dashed box.

In this system, the basic solution (ammonia-water mixture) becomes a vapor-liquid two-phase mixture (1) after heat exchange with geothermal water in the generator, then leaves the generator as a saturated mixture and enters the separator afterward. Ammonia vapor (2) separated from the top of the separator is expanded in the turbine to generate power, and ammonia-poor solution (13) separated from the bottom of the separator flows through the high-temperature (HT) recuperator (14) and throttle (15) to be cooled and depressurized to 15 bar, respectively. At the same time, turbine exhaust (3) is split into two streams, and the split ratio is 1:1. One of the two streams (9) is cooled to be saturated liquid (10) in the second condenser (SC) and pressurized (11) to be middle pressure (15 bar) in the second cooling pump (SCP) and then enters into the evaporator to recycle the remaining energy content of geothermal water in the second evaporator (SE), which has heat exchange with the basic solution in the generator. Then, stream (15) is mixed with stream (12) in the first mixture commingler (FMC), which is adiabatic. The mixing process of ammonia-water is an exothermic process, but to simplify the calculation program, it is only a mixing process without an exothermic process in FMC while exothermic in the absorber. Stream (16) enters the absorber to release dissolution heat, which is absorbed by the low-temperature basic solution (17). At the same time, the other stream (18) of turbine exhaust is diluted with stream (4) in the second mixture commingler (SMC), which is adiabatic and condensed (4,5,6) in the low-temperature (LT) recuperator and the first condenser (FC) by the low-temperature basic solution and cooling water, respectively. The saturated basic solution (6) leaving FC is pressurized to high pressure (32.3 bar) in the first cooling pump (FCP). Then, the high-pressure basic solution is sent to the LT recuperator (8), absorber (19), and HT recuperator (20) to recycle thermal energy from the high-temperature solution. Finally, the basic solution (1) enters the generator, and the whole process starts again.

The absorption heat transformer subsystem is the key component for MKC. The advantages of MKC are mainly shown in two aspects. First, the benefit comes from the absorption heat transformer subsystem because the remaining energy content of the geothermal water that has heat exchange with basic solution in the generator can be recycled by condensed turbine exhaust, and the temperature of the final discharged tail water is decreased. Second, the dissolution heat released in the absorber can be absorbed by the low-temperature basic solution to increase the generator inlet temperature of the basic solution, which leads to a higher mass flow of ammonia vapor, and increased net power output. Considering the amount of electricity generated, the modified system

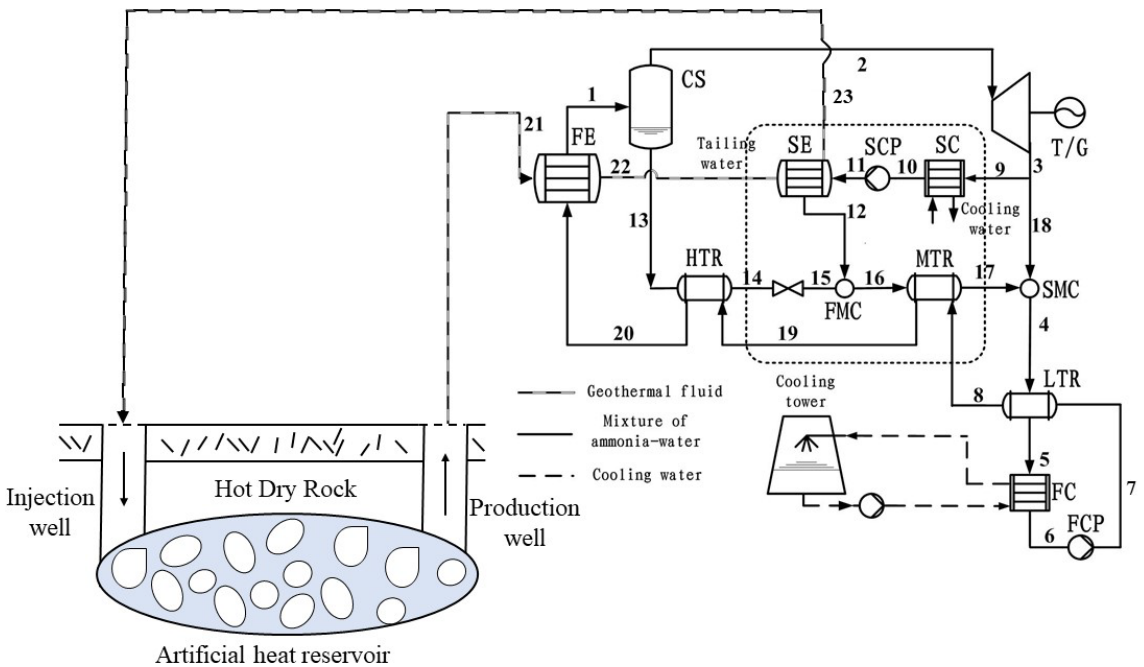

Figure 2. Schematic diagram of MKC.

attempts to demonstrate the technical and economic feasibility of extracting energy from geothermal resources.

2.2. Modeling

According to the actual parameters of the Kalina cycle power plant, the system results are calculated by Engineering Equation Solver (EES) software, and the input parameters in each unit of the MKC can be confirmed, as shown in Table 1. The basic models for all units involve mass, energy, and component conservation equations. To simplify the calculation, the following assumptions are made in this paper:

a) The cycle is operated under a steady state all the time.

b) The turbine and pumps have isentropic efficiencies.

c) There is no pressure drop along the pipeline.

d) The power consumption of the cooling water pump is neglected.

The theoretical calculation equations in each unit of the Kalina cycle are shown in Table 2 (a), and the theoretical calculation equations in each unit of the MKC are shown in Table 2 (b). The basic models for all units involve mass, energy, and component conservation equations.

In the equations shown above, Q represents energy, kJ; m represents mass flow of solution, kg/s; x represents ammonia concentration; W represents power, kW; η represents thermal efficiency; h represents enthalpy, kJ/kg; s represents entropy, kJ/kg; p represents pressure, bar; v represents specific volume, m^3/kg.

3. Results and discussion

3.1. Validation

The same input parameters and operating conditions of the Kalina cycle studied previously (Ogriseck, 2009) are adopted in this paper, as shown in Table 1. Under the same boundary conditions, the comparison of the main parameters in the Kalina Power Plant in Husavik, the Kalina cycle in a previous study (Ogriseck, 2009) and MKC in this paper are shown in Table 3 and Table 4. In Table 3, the simulation results of the Kalina cycle have been validated with the results in the references (Kalina et al., 1991; Marston et al., 1994). The parameters of each point of the system are basically consistent with the measured values in the references. It can be considered that this model is correct; therefore, we show the MKC state point parameters in Table 4.

A simple way to evaluate the alternative power cycles during preliminary power cycle design is to compare the performance of any new proposed cycle that produces the power output under the same conditions, so the thermodynamic parameters listed in Table 5 between Kalina and MKC are made with the same conditions. Comparing the total output power of MKC and Kalina cycle, it can be found that the total power output of Kalina cycle is lower than that of the MKC cycle under the same conditions. The work output increases by 221 kW, approximately 10.5%, and the detailed data are shown in Table 5. Because tailwater adopts a greater temperature drop, the MKC is designed to use the heat of geothermal fluid from 122 °C to 60 °C and only 122 °C to 80 °C for the Kalina cycle. Therefore, MKC absorbs more heat from geothermal water than KSC, leading to greater net power. However, the thermal efficiency of MKC cycle is lower. This is because compared to the Kalina cycle, the extra heat of MKC absorbed is the temperature of geothermal water in the range of 60–80 °C. The power efficiency of the Kalina cycle when the source temperature in this range is lower than when the source temperature is in the range of 80–122 °C. Therefore, the total power efficiency of MKC is lower than that of the Kalina cycle. However, under the same mass flow of geothermal water, MKC has a greater net power. So, MKC has a better performance than the Kalina cycle.

3.2. Discussion

The corresponding thermodynamic model is built to investigate the system performance. The ammonia-water

Table 1. Input parameters of MKC.

Items	Parameters	Items	Parameters
Temperature of geothermal water/°C	122	High pressure/bar	32.3
Temperature of middle tail water/°C	80	Turbine isentropic efficiency	0.87
Temperature of final tail water/°C	60	Generation efficiency	0.96
Cooling water inlet temperature/°C	5	Pump isentropic efficiency	0.98
Mass flow of geothermal water/kg/s	89	Split ratio of turbine exhaust	1:1
Ammonia content of basic solution	0.82	Middle pressure/bar	15
Minimum temperature difference of generator/°C	6	Minimum temperature difference of evaporator/°C	6
Minimum temperature difference of recuperator/°C	5	Minimum temperature difference of condenser/°C	3
Pressure drop of heat exchanger/bar	1	Pressure drop of pipeline/bar	0

Table 2. (a). Theoretical calculation equations of the KSC.

Project	Equation	NO.
Energy conservation equation	$\Delta_{out}^{in} \sum_i Q_i = 0$	(1)
Mass conservation equation	$\Delta_{out}^{in} \sum_i m_i = 0$	(2)
Generator	$m_{gen} \cdot (h_{13} - h_{14}) = m_{basic} \cdot (h_5 - h_4)$	(3)
Separator	$m_{basic} = m_6 + m_7$ $m_5 \cdot x_{basic} = m_6 \cdot x_6 + m_7 \cdot x_7$	(4) (5)
Steam turbine	$W_{tur} = m_6 \cdot (h_6 - h_{10}) \cdot \eta_{i\_1}$ $\eta_{i\_1} = \frac{(h_6 - h_{10})}{(h_6 - h_{10s})}$	(6) (7)
High temperature regenerator	$m_7 \cdot (h_7 - h_8) = m_4 \cdot (h_4 - h_{12})$	(8)
Low temperature regenerator	$m_1 \cdot (h_1 - h_{11}) = m_{12} \cdot (h_{12} - h_3)$	(9)
Condenser	$Q_{cond} = m_{basic} \cdot (h_9 - h_{10})$	(10)
Working fluid pump	$s_2 = s_3$ $W_{pump} = \frac{m_{basic} \cdot v_2 \cdot (p_3 - p_2) \cdot 100}{\eta_{pump\_ksc}}$	(11) (12)
Mixer	$m_1 = m_8 + m_{10}$ $m_1 \cdot x_1 = m_8 \cdot x_8 + m_{10} \cdot x_{10}$ $m_1 \cdot h_1 = m_8 \cdot h_8 + m_{10} \cdot h_{10}$	(13) (14) (15)

concentration, inlet pressure, and temperature of heat sources are necessary to analyze because operating states should be changed. The dynamic power output of the turbine is selected to be an objective function to compare and optimize the system performance under satisfactory separation conditions.

3.2.1. Limit range

It is difficult to condense the turbine exhaust completely because the ammonia concentration of the turbine exhaust is too high (0.97) and is almost pure ammonia vapor. Consequently, the temperature of the bubble point is low, and the turbine exhaust can only be condensed to liquid completely by cooling water with a temperature lower than the bubble point. The high cooling water temperature requirement caused large limitations on MKC application in general regions. The temperature of the cooling water used in the simulation is only 5 °C and can complete the condensation process perfectly. However, the temperature of cooling water, is not easy to obtain in general regions throughout the year and always changes with season. Consequently, the limit caused by the cooling water cannot be ignored.

In MKC, the ammonia concentration at point 20 in Figure 3 is 0.82. When the temperatures of cooling water are changed from 5 °C to 30 °C, the pressures of the condensed turbine exhaust that flow out the FC are changed from 5.769 bar to 11.21 bar, which leads to the temperatures of bubble point being changed from 8.39 °C to 29.73 °C as shown in Figure 3. When the temperature of cooling water is lower than 8 °C, the minimum temperature difference of FC is higher than 3 °C, which meets the assumption used during the simulation. Once the cooling water temperature is higher than 8 °C, it will become more difficult to condense the turbine exhaust completely and cause a higher requirement on the condenser, which limits MKC application, especially in summer.

To avoid this limit, some measures are necessary to increase the temperature of the bubble point, such as changing the ammonia concentration at point 20. During the simulation, the pressure of the turbine exhaust would increase with increasing ammonia concentration, which leads to an increase in bubble point temperature. Consequently, it is possible to adopt a higher cooling water temperature to complete the condensation process.

Table 2. (b). Theoretical calculation equations of the MKC.

Project	Equation	NO.
Generator	$m_{gen} \cdot (h_{21} - h_{22}) = m_1 \cdot (h_1 - h_{20})$	(1)
Separator	$m_1 = m_2 + m_{13}$ $m_1 \cdot h_1 = m_2 \cdot h_2 + m_3 \cdot h_3$	(2) (3)
Steam turbine	$W_{tur} = m_2 \cdot (h_2 - h_3) \cdot \eta_{i\_2}$ $\eta_{i\_2} = \frac{(h_2 - h_3)}{(h_2 - h_{3s})}$	(4) (5)
Evaporator	$m_{gen} \cdot (h_{22} - h_{23}) = m_9 \cdot (h_{12} - h_{11})$	(6)
High temperature regenerator	$m_{13} \cdot (h_{13} - h_{14}) = m_{19} \cdot (h_{20} - h_{19})$	(7)
Low temperature regenerator	$m_4 \cdot (h_4 - h_5) = m_8 \cdot (h_8 - h_7)$	(8)
Condenser 1st	$Q_{cond\_1} = m_5 \cdot (h_5 - h_6)$	(9)
Condenser 2st	$Q_{cond\_2} = m_9 \cdot (h_9 - h_{10})$	(10)
Working fluid pump 1st	$s_6 = s_7$ $W_{pump\_1} = \frac{m_6 \cdot v_6 \cdot (p_7 - p_6) \cdot 100}{\eta_{pump}}$	(11) (12)
Working fluid pump 2st	$s_{10} = s_{11}$ $W_{pump\_2} = \frac{m_{10} \cdot v_{10} \cdot (p_{11} - p_{10}) \cdot 100}{\eta_{pump}}$	(13) (14)
Mixer	$m_4 = m_{17} + m_{18}$ $m_4 \cdot x_4 = m_{17} \cdot x_{17} + m_{18} \cdot x_{18}$ $m_4 \cdot h_4 = m_{17} \cdot h_{17} + m_{18} \cdot h_{18}$	(15) (16) (17)
Absorber	$m_{16} = m_{12} + m_{15}$ $m_{16} \cdot x_{16} = m_{12} \cdot x_{12} + m_{15} \cdot x_{15}$ $m_{16} \cdot h_{16} = m_{12} \cdot h_{12} + m_{15} \cdot h_{15}$	(18) (19) (20)
Thermal efficiency	$Q_{geo\_1} = m_{geo} \cdot (h_{21} - h_{22})$ $Q_{geo\_2} = m_{geo} \cdot (h_{22} - h_{23})$ $Q_{total} = Q_{geo\_1} + Q_{geo\_2}$ $W_{net} = W_{tur} - W_{pump\_1} - W_{pump\_2}$ $\eta = \frac{W_{net}}{Q_{total}}$	(21) (22) (23) (24) (25)

When the ammonia concentration was 0.9, the pressure of the condensed turbine exhaust that flowed out of the FC changed from 6.13 bar to 12.52 bar, and the cooling water temperatures changed from 5 °C to 30 °C. At the same time, the temperatures of the bubble point that flowed out the FC changed from 10.81 °C to 33.49 °C. It is obvious that the minimum temperature difference of FC is higher than 3 °C in the whole range of cooling water temperatures, which meets the assumption and breaks the limit caused by the cooling water temperature. Therefore, for general regions, the ammonia water mixture with a concentration of 0.9 is the optimal concentration under the simulated heat source and pressure, rather than the 0.82 ammonia water mixture used in Iceland.

Table 3. Main parameters of the Kalina cycle system.

No.	T (°C)		P (bar)		Vapor fraction		x	
	Simulation	Ref.	Simulation	Ref.	Simulation	Ref.	Simulati-on	Ref.
1	45.9	46	6.77	6.6	0.82	0.82	0.63	0.64
2	7.9	8	4.77	4.6	0.82	0.82	0	0
3	8.1	8	35.3	35.3	0.82	0.82	0	0
4	62.5	63	33.3	33.3	0.82	0.82	0	0
5	116	116	32.3	32.3	0.82	0.82	0.67	0.68
6	116	116	32.3	32.3	0.972	0.97	1	1
7	116	116	32.3	32.3	0.511	0.50	0	0
8	44.7	46	31.3	31.3	0.511	0.50	0	0
9	45.1	—	6.77	—	0.511	—	0	—
10	42.1	43	6.77	6.6	0.972	0.97	0.944	0.94
11	29.7	30	5.77	5.6	0.82	0.82	0.543	0.56
12	39.7	41	34.3	34.3	0.82	0.82	0	0
13	122	122	—	—	—	—	—	—
14	80	80	—	—	—	—	—	—

Note: (Ref. is the reference (Marston et al., 1994)).

Table 4. Results of MKC.

No.	T (°C)	P (bar)	Vapor fraction	x
1	116	32.3	0.82	0.6708
2	116	32.3	0.9718	1
3	42.33	6.769	0.9718	0.944
4	40.62	6.769	0.82	0.5923
5	28.28	5.769	0.82	0.5273
6	8	4.769	0.82	0
7	8.428	36.3	0.82	0
8	35.38	35.3	0.82	0
9	42.33	6.769	0.9718	0.944
10	8.934	5.769	0.9718	0
11	9.009	8.769	0.9718	0
12	52.79	7.769	0.9718	0.9538
13	116	32.3	0.5107	0
14	60.75	31.3	0.5107	0
15	61.05	14	0.5107	0
16	55.6	7.769	0.7434	0.5
17	40.38	6.769	0.7434	0.4136
18	42.33	6.769	0.9718	0.944
19	59.02	34.3	0.82	0
20	74	33.3	0.82	0
21	122	——	——	——
22	80	——	——	——
23	60	——	——	——

Table 5. Comparison results.

Parameters	KCS	MKC
Work output	2108 kW	2329 kW
First pump power	74.38 kW	101 kW
Second pump power	——	3.57 kW
Efficiency, Z (%)	13.43	9.42

3.2.2. Effect of cooling water temperature

The cooling water temperature of 5 °C adopted during the simulation process is derived from reference (Ogriseck, 2009). However, for general regions, such a low cooling water temperature is not easy to obtain throughout the year. In China, the annual average temperature is approximately 20 °C, and the cooling water temperature changes seasonally. Therefore, research on cooling water temperature is necessary.

In this article, a cooling water temperature of 5 °C ~30 °C is selected as the research object. At the same time, according to the discussion shown above, only one kind of concentration (0.9) is selected to analyze the effect of cooling water temperature. The simulation result is shown in Figure 4 in which the turbine exhaust pressure is increased, and the net power output is decreased almost straight with increasing cooling water temperature. For example, when the ammonia concentration of the basic

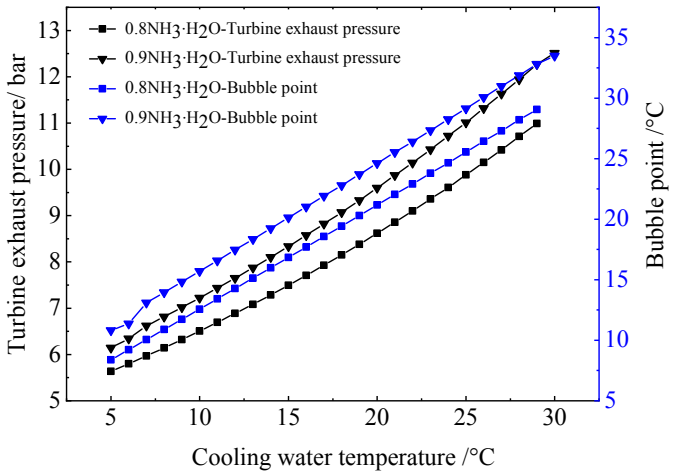

Figure 3. Limit of cooling water temperature.

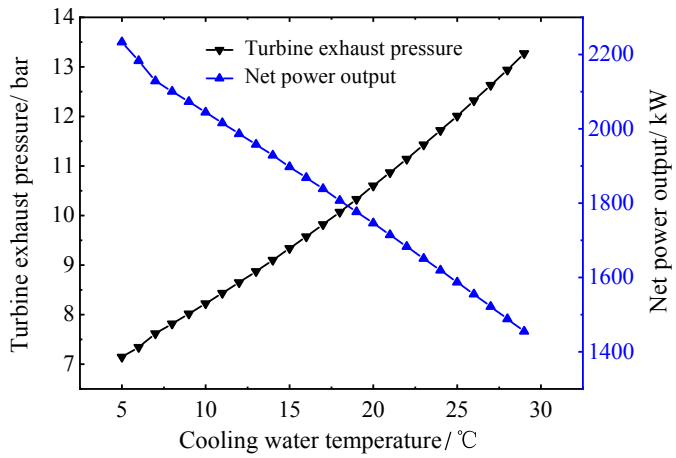

Figure 4. Effect of cooling water temperature.

solution is 0.9 and the cooling water temperature is decreased from 30 °C to 5 °C, the turbine exhaust pressure is decreased from 13.3 bar to 7.1 bar, and the net power output is increased by 53.5%. It also reveals that different cooling water temperatures correspond to different optimum turbine exhaust pressures. In China, when the power plant is operated with a cooling water temperature of 20 °C throughout the year, the optimum turbine exhaust pressure is approximately 10.6 bar, and the net power output and thermal efficiency are approximately 1746.1 kW and 7.52%, respectively.

3.2.3. Effect of ammonia concentration

The ammonia concentration of the basic solution is a key parameter that directly affects the mass flow of ammonia vapor. It is important to study the effect of the concentration of the basic solution and seek the optimum ammonia concentration under certain conditions.

Four kinds of turbine inlet pressures are selected, and the results are shown in Figure 5 (a). The trend of net power output is that it increases sharply first and then decreases gradually with increasing ammonia concentration. This is mainly caused by two reasons, as shown in Figures 5 (b) and 5 (c). First, with increasing ammonia concentration, there is a better match between the basic solution and heat source during the heat transfer process in the generator, which leads to a lower irreversible loss, and more ammonia vapor can be generated to expand in the turbine. Consequently, the net power output is increased sharply. Second, the ammonia concentration cannot be too high. The advantage of variable evaporation temperature will be weakened if the concentration is close to 100% because the ammonia-water mixture is almost pure quality, which leads to a high irreversible loss, as shown in Figure 5 (b). Additionally, the enthalpy difference of ammonia vapor that flows through the turbine is decreased, which leads to

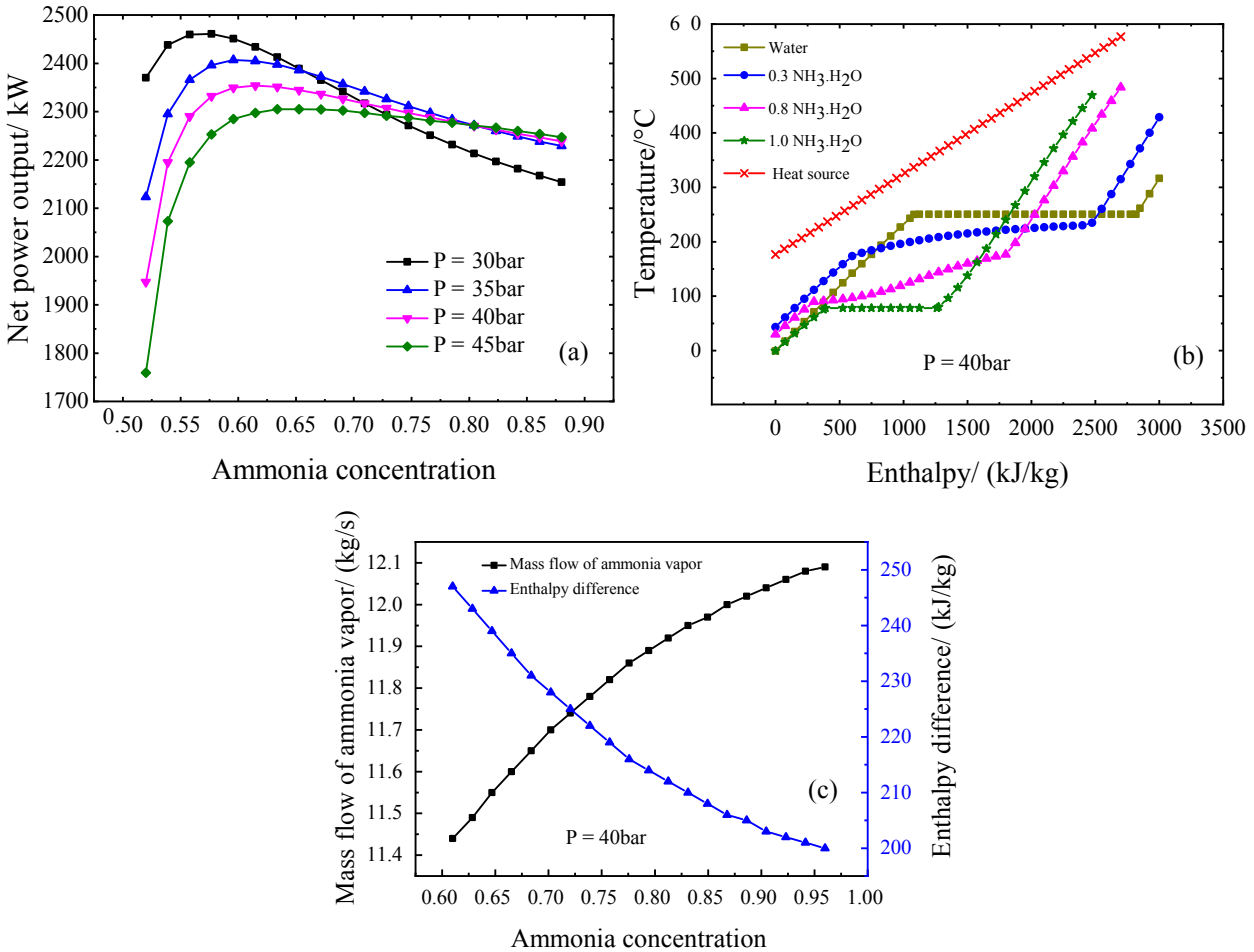

Figure 5. (a) Ammonia concentration and net power output, (b) heat transfer process between different concentrations of basic solution and heat source, (c) ammonia concentration and ammonia vapor.

a decrease in power output, as shown in Figure 5 (c). The synthetic action results in a changing trend, as shown in Figure 5 (a).

At the same time, the optimum ammonia concentration exists under a certain turbine inlet pressure. When the turbine inlet pressures are 30 bar, 35 bar, 40 bar and 45 bar, the optimum ammonia concentrations are 0.59, 0.64, 0.70 and 0.79, respectively. It obviously shows that the optimum ammonia concentration increases with increasing turbine inlet pressure.

3.2.4. Effect of turbine inlet pressure

Under the condition of constant cooling water temperature, the turbine exhaust pressure is constant. The net power output is only related to the turbine inlet pressure. At the same time, the mass flow of the basic solution and the power consumption of the feed pumps have a relationship with the turbine inlet pressure. In addition, the optimum pressure is different with the change in ammonia concentration. Consequently, it is necessary to study the effect of turbine inlet pressure.

Four kinds of basic solutions with different concentrations are selected, and the results are shown in Figure 6. As shown in Figure 6 (a), the net power output increases first and then decreases with increasing turbine inlet pressure. On the one hand, with the increase in turbine inlet pressure, the mass flow of the basic solution is increased sharply, as shown in Figure 6 (b), which can lead to a higher mass flow of ammonia vapor. Additionally, the power output is increased with the increase in the pressure ratio within a certain limit. On the other hand, the mass flow of ammonia vapor generated in the generator will be limited if the turbine inlet pressure is beyond the optimum pressure, and the power consumption of feed pumps has a corresponding increase with the increase in turbine inlet pressure, as shown in Figure 6 (c), which leads to a decrease in net power output. Both reasons result in such a trend, as shown in Figure 6 (a).

In addition, the corresponding optimum pressures are 29 bar, 36 bar, 41 bar, and 45 bar when the ammonia concentrations of the basic solution are 0.6, 0.7, 0.8, and 0.9,

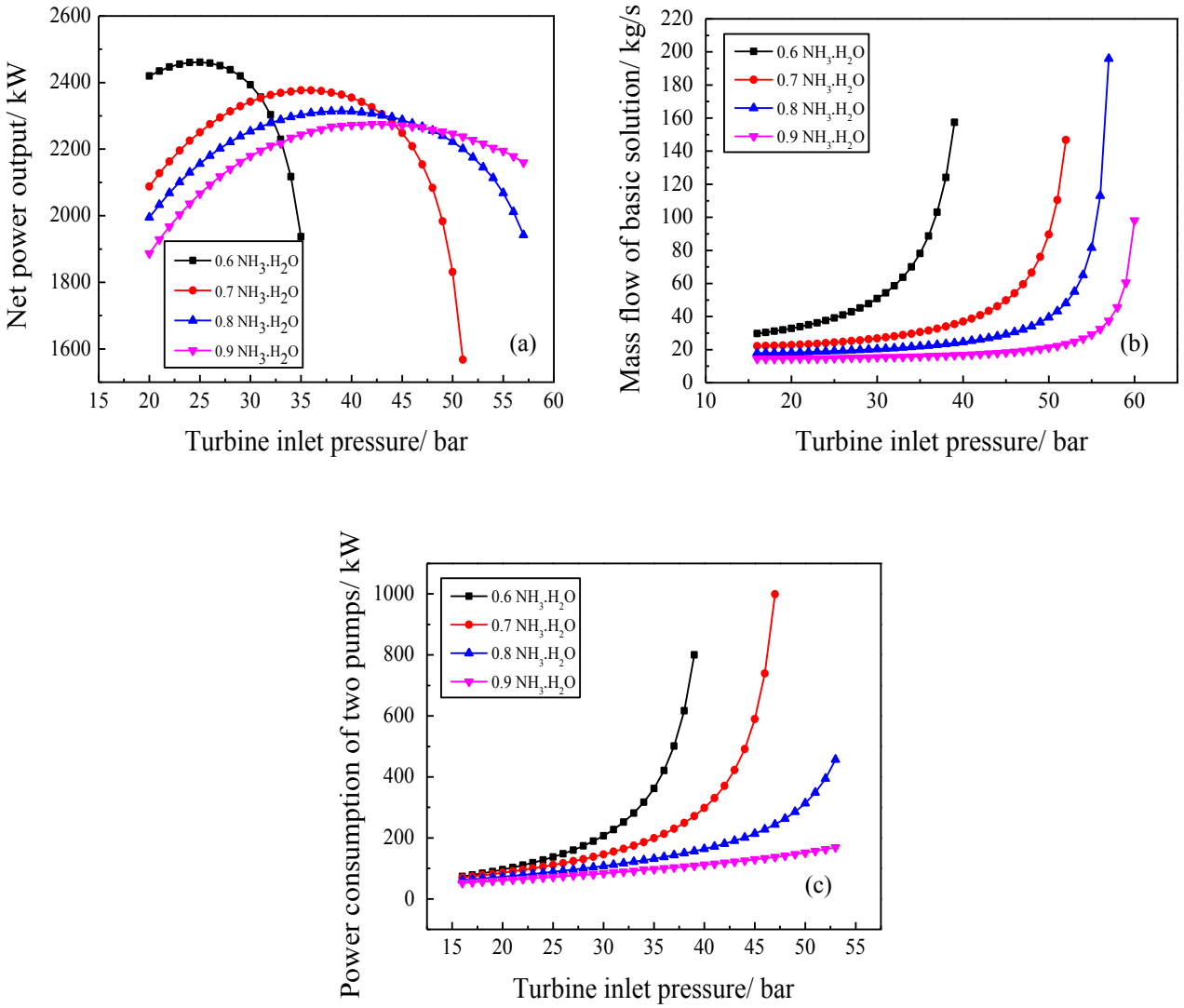

Figure 6. (a) Turbine inlet pressure and net power output, (b) turbine inlet pressure and mass flow of the basic solution, and (c) turbine inlet pressure and power consumption of the two pumps.

respectively. It obviously shows that the optimum pressure is increased with increasing ammonia concentration. The optimum turbine inlet pressure exists to guarantee the highest net power output under certain conditions.

4. Conclusion

To improve the utilization rate of HDR resources, a modified power cycle is proposed and analyzed in this paper. The results show that the performance of MKC is improved compared to that of the Kalina cycle in a previous study (Ogriseck, 2009) under the same conditions. Based on the simulation results, the following conclusions can be drawn:

(1) The net power output of MKC is infcreased by 10.5% compared to that of the Kalina cycle. It should be noted that MKC can use more heat energy to generate electricity.

(2) In general regions, to avoid the application limit caused by cooling water, the best ammonia concentration is 0.9 under the heat source and pressure used in the simulation.

(3) The lower the cooling water temperature is, the lower the turbine exhaust pressure and the higher the net power output.

(4) Different ammonia concentrations have different optimal turbine inlet pressures. For ammonia concentrations of the basic solution of 0.6, 0.7, 0.8 and 0.9, the optimum pressures are 29 bar, 36 bar, 41 bar and 45 bar, respectively.

The results of this study will contribute to the construction of a demonstration project for HDRs in China and their efficient utilization.

Acknowledgments
The authors gratefully acknowledge the financial support provided by the National Key R & D Program of China (2018YFB1501801-04) and the State Grid Qinghai Electric Power Company Science and Technology Project: Hot dry rock power generation and industrial development to Qinghai New Energy Support Capacity Research (52280719004F).

References

Bo HL, Liu XD, Liu GY (1989). Calculating method for thermodynamic properties of water and ammonia mixture. Journal of Xian Jiaotong University 23 (3): 49-56 (article in Chinese with an abstract in English).

Bo HL, Liu XD, Liu GY (1989). Thermodynamic analysis for Kalina cycle. Journal of Xian Jiaotong University 23 (3): 57-63 (article in Chinese with an abstract in English).

Chen SY, Hua JY, Chen YP, Wu JF (2012). Thermal performance of triple pressure ammonia-water power cycle for waste heat recovery. Journal of Southeast University 42 (4): 659-663 (article in Chinese with an abstract in English).

El-sayed Tribus (1985). Theoretical comparison of the Rankine and Kalina cycles. In: Analysis of Energy Systems-Design and Operation 97-102.

Fang SQ, Luo PM (2008). The research and application of the absorption heat transformer. Applied Energy Technology 10: 36-39.

Fu WC, Zhu JL, Zhang W, Lu ZY (2013). Performance of evaluation of Kalina cycle subsystem on geothermal power generation in the oilfield. Applied Thermal Engineering 54: 497-506.

Gao Q, Zheng DX, Jiang CS (1993). Study on working pairs for absorption heat transformers. Petrochemical Technology 22: 382-392.

Hettiarachchi HDM, Golubovic M, Worek WM, Ikegamiet Y (2007). The Performance of the Kalina Cycle System 11(KCS11) With Low-Temperature Heat Sources. Journal of Energy Resources Technology 129 (3).

Huang T, Dong HH (2008). Research of the absorption heat transformer for recovering the geothermal waste heat. Refrigeration and Air Conditioning 22 (1): 43-48.

Kalina Leibowitz, Markus Pelletier (1991). Further technical aspects and economics of a utility-size Kalina bottoming cycles. In: International Gas Turbine and Aeroengine Congress and Exposition 4: 1-8.

Li DW, Wang YX (2015). Major Issues of Research and Development of Hot Dry Rock Geothermal Energy. Earth Science (Journal of China University of Geosciences) 40 (11): 1858-1869 (article in Chinese with an abstract in English).

Liu M, Zhang N, Cai RX (2006). A series connected ammonia absorption power/refrigeration combined cycle. Journal of engineering thermophysics 27 (1): 9-12.

Liu QW, Yin HC (2012). Performance analysis on NH3/H2O absorption refrigeration using pinch methods. Energy Conservation 7: 33-35.

Lu L, Yan JY, Ma YT, Lu CR (1989). Thermodynamic analysis of heat-releasing process of Kalina cycle. Journal of Engineering Thermophysics 10 (3): 249-251 (article in Chinese with an abstract in English).

Marston, Charles H, Sanyal, Yoddhojit (1994). Optimization of Kalina cycles for geothermal applications. In: Proceedings of the 1994 International Mechanical Engineering Congress and Exposition 97-100.

Nasruddin, Rama U, Maulana R, Agus N (2009). Energy and exergy analysis of kalina cycle system (KCS) 34 with mass fraction ammonia-water mixture variation. Journal of Mechanical Science & Technology 23: 1871–1876.

Ogriseck S (2009). Integration of Kalina cycle in a combined heat and power plant, a case study. Applied Thermal Engineering 29 (14-15): 2843-2848.

Wang JF, Wang JQ, Dai YP (2008). Study on the application of Kalina cycle in the middle and low temperature waste heat recovery. Turbine Technology 50 (3): 208-210 (article in Chinese with an abstract in English).

Wu XH, Chen B, Zheng DX (2003). Thermodynamic analysis of ammonia-water absorption refrigeration cycle. Journal of North China Electric Power University 30 (5): 66-69.

Wei GS, Meng J, Du XZ, Yang YP (2015). Performance analysis on a hot dry rock geothermal resource power generation system based on Kalina cycle. In: The 7th International Conference on Applied Energy 937-945.

Xu F, Goswami DY, Bhagwat SS (2014). A combined power/cooling cycle. Energy 25 (4): 233-246.

Zhang Y, He MG, Jia Z, Liu X (2007). An analysis of Kalina cycle based on the 1st law of thermodynamic. Journal of Power Engineering 27 (2): 218-222 (article in Chinese with an abstract in English).

Zheng DX, Chen B, Qi Y, Jin HG (2002). A thermodynamic analysis of a novel absorption power/cooling combined cycle. Journal of Engineering Thermophysics 23 (5): 539-542 (article in Chinese with an abstract in English).

Zheng SP, Zheng DX (2005). Ammonia absorption cycle by solar energy and geothermal energy. Acta Energiae Solaris Sinica 26 (4): 513-517.